

# Preparation, characterization, and catalytic activity of bismuth molybdate catalysts for the oxidative dehydrogenation of *n*-butene into 1,3-butadiene

Ji Chul Jung<sup>a</sup>, Heesoo Kim<sup>a</sup>, Ahn Seop Choi<sup>b</sup>, Young-Min Chung<sup>b</sup>, Tae Jin Kim<sup>b</sup>,  
Seong Jun Lee<sup>b</sup>, Seung-Hoon Oh<sup>b</sup>, In Kyu Song<sup>a,\*</sup>

<sup>a</sup> School of Chemical and Biological Engineering, Institute of Chemical Processes, Seoul National University,  
Shinlim-dong, Kwanak-ku, Seoul 151-744, South Korea

<sup>b</sup> SK Corporation, Yuseong-ku, Daejeon 305-712, South Korea

Received 17 April 2006; received in revised form 8 June 2006; accepted 9 June 2006  
Available online 24 July 2006

## Abstract

Three types of bismuth molybdate catalysts,  $\alpha$ -Bi<sub>2</sub>Mo<sub>3</sub>O<sub>12</sub>,  $\beta$ -Bi<sub>2</sub>Mo<sub>2</sub>O<sub>9</sub>, and  $\gamma$ -Bi<sub>2</sub>MoO<sub>6</sub>, were prepared by a co-precipitation method for use in the oxidative dehydrogenation of *n*-butene. Unlike  $\alpha$ -Bi<sub>2</sub>Mo<sub>3</sub>O<sub>12</sub> and  $\gamma$ -Bi<sub>2</sub>MoO<sub>6</sub>, it was found that  $\beta$ -Bi<sub>2</sub>Mo<sub>2</sub>O<sub>9</sub> was thermally unstable and decomposed into  $\alpha$ -Bi<sub>2</sub>Mo<sub>3</sub>O<sub>12</sub> and  $\gamma$ -Bi<sub>2</sub>MoO<sub>6</sub> at the reaction temperature of 420 °C. Therefore,  $\beta$ -Bi<sub>2</sub>Mo<sub>2</sub>O<sub>9</sub> could not serve as an efficient catalyst in the reaction. In the oxidative dehydrogenation of *n*-butene into 1,3-butadiene,  $\gamma$ -Bi<sub>2</sub>MoO<sub>6</sub> showed a better catalytic performance than  $\alpha$ -Bi<sub>2</sub>Mo<sub>3</sub>O<sub>12</sub>. The different catalytic performance between  $\alpha$ -Bi<sub>2</sub>Mo<sub>3</sub>O<sub>12</sub> and  $\gamma$ -Bi<sub>2</sub>MoO<sub>6</sub> catalysts was elucidated by temperature-programmed reoxidation (TPRO) experiments. It was revealed that the enhanced catalytic performance of  $\gamma$ -Bi<sub>2</sub>MoO<sub>6</sub> was attributed to the facile oxygen mobility of  $\gamma$ -Bi<sub>2</sub>MoO<sub>6</sub>.

© 2006 Elsevier B.V. All rights reserved.

**Keywords:** Bismuth molybdate; *n*-Butene; 1,3-Butadiene; Oxidative dehydrogenation; Oxygen mobility; Temperature-programmed reoxidation (TPRO)

## 1. Introduction

1,3-Butadiene has attracted much attention as a raw material for styrene butadiene rubber (SBR), polybutadiene rubber (BR), and acrylonitrile butadiene styrene (ABS) in the petrochemical industries [1]. Steam cracking [2], direct dehydrogenation of *n*-butene [3–5], and oxidative dehydrogenation of *n*-butene [6–9] are well known processes used for the production of 1,3-butadiene. Steam cracking, the major manufacturing process for 1,3-butadiene, involves many problems in both marketing and energy management, because steam cracking produces not only 1,3-butadiene but also many petrochemical raw materials such as ethylene, propylene, and isobutene, simultaneously [2]. Direct dehydrogenation of *n*-butene into 1,3-butadiene is thermodynamically unfavorable and requires

high reaction temperature [2–4]. However, oxidative dehydrogenation of *n*-butene into 1,3-butadiene is thermodynamically favorable and requires low reaction temperature [6–9], compared to direct dehydrogenation of *n*-butene. Therefore, oxidative dehydrogenation of *n*-butene has been recognized as a promising process that can produce 1,3-butadiene in a single unit [6–9].

Bismuth molybdates have been widely investigated as efficient catalysts for the oxidative dehydrogenation of *n*-butene [6–9]. Typically, three types of bismuth molybdate catalysts,  $\alpha$ -Bi<sub>2</sub>Mo<sub>3</sub>O<sub>12</sub>,  $\beta$ -Bi<sub>2</sub>Mo<sub>2</sub>O<sub>9</sub>, and  $\gamma$ -Bi<sub>2</sub>MoO<sub>6</sub>, have been considered for this reaction [7,10–12]. However, it is known that  $\beta$ -Bi<sub>2</sub>Mo<sub>2</sub>O<sub>9</sub> is thermally unstable at temperatures ranging from 400 to 550 °C [7,13]. Therefore, major studies on the oxidative dehydrogenation of *n*-butene have been focused on the  $\alpha$ -Bi<sub>2</sub>Mo<sub>3</sub>O<sub>12</sub> and  $\gamma$ -Bi<sub>2</sub>MoO<sub>6</sub> catalysts. It is also known that the catalytic performance of bismuth molybdate in the oxidative dehydrogenation of *n*-butene strongly depends on the oxygen mobility of the catalyst [7,14,15]. It is expected that a catalyst

\* Corresponding author. Tel.: +82 2 880 9227; fax: +82 2 888 7295.  
E-mail address: [inksong@snu.ac.kr](mailto:inksong@snu.ac.kr) (I.K. Song).

with high oxygen mobility may show an excellent catalytic performance in this reaction [6,14–18].

In this work,  $\alpha$ -Bi<sub>2</sub>Mo<sub>3</sub>O<sub>12</sub>,  $\beta$ -Bi<sub>2</sub>Mo<sub>2</sub>O<sub>9</sub>, and  $\gamma$ -Bi<sub>2</sub>MoO<sub>6</sub> were prepared by a co-precipitation method for use in the oxidative dehydrogenation of *n*-butene. The prepared catalysts were characterized by XRD, BET, Raman spectroscopy, and ICP-AES analyses. Thermal stability of the catalysts was also investigated. Oxygen mobility of the catalyst was measured by temperature-programmed reoxidation (TPRO) experiment to elucidate the catalytic performance.

## 2. Experimental

### 2.1. Preparation of bismuth molybdate catalysts

Bismuth molybdate catalysts were prepared by a co-precipitation method. Known amount of bismuth nitrate (Bi(NO<sub>3</sub>)<sub>3</sub>·5H<sub>2</sub>O) was dissolved in distilled water which was acidified with concentrated nitric acid. The solution was then added dropwise into the aqueous solution containing known amount of ammonium molybdate ((NH<sub>4</sub>)<sub>6</sub>Mo<sub>7</sub>O<sub>24</sub>·4H<sub>2</sub>O) under vigorous stirring. During the co-precipitation step, pH of the mixed solution was precisely controlled by adjusting the amount of ammonia solution added. The pH values were kept at 1.5, 5.0, and 3.0 in the preparation of  $\alpha$ -Bi<sub>2</sub>Mo<sub>3</sub>O<sub>12</sub>,  $\beta$ -Bi<sub>2</sub>Mo<sub>2</sub>O<sub>9</sub>, and  $\gamma$ -Bi<sub>2</sub>MoO<sub>6</sub>, respectively [6,19]. After the resulting solution was stirred vigorously at room temperature for 1 h, the precipitate was filtered to obtain a solid product. The solid product was dried overnight at 110 °C, and then it was calcined at 475 °C for 5 h to yield the bismuth molybdate catalyst.

### 2.2. Characterization

Formation of pure  $\alpha$ -Bi<sub>2</sub>Mo<sub>3</sub>O<sub>12</sub>,  $\beta$ -Bi<sub>2</sub>Mo<sub>2</sub>O<sub>9</sub>, and  $\gamma$ -Bi<sub>2</sub>MoO<sub>6</sub> was confirmed by XRD (MAC Science, M18XHF-SRA) and Raman spectroscopy (Horiaba Jobin Yvon, T64000) measurements. Bi/Mo atomic ratios of the prepared catalysts were determined by ICP-AES (Shimadzu, ICP-1000IV) analyses. Surface areas of the catalysts were measured using an ASAP 2010 instrument (Micromeritics). In order to measure the oxygen mobility of the catalysts, temperature-programmed reoxidation (TPRO) experiments were carried out. For the TPRO experi-

ment, each catalyst was partially reduced by carrying out the oxidative dehydrogenation of *n*-butene without oxygen feed at 420 °C for 3 h. After the reduced catalyst was placed in a conventional TPRO apparatus, a mixed stream of oxygen (10%) and helium (90%) was introduced to the catalyst sample. Furnace temperature was raised from room temperature to 500 °C at a heating rate of 5 °C/min. The amount of oxygen consumed was detected using a thermal conductivity detector.

### 2.3. Oxidative dehydrogenation of *n*-butene

Oxidative dehydrogenation of *n*-butene into 1,3-butadiene was carried out in a continuous flow fixed-bed reactor. Feed composition was fixed at *n*-butene:oxygen = 1:0.75. C<sub>4</sub> raffinate-3 containing 72.5 wt% *n*-butene (1-butene(14.2 wt%) + *trans*-2-butene(38.3 wt%) + *cis*-2-butene(20.0 wt%)) was used as a *n*-butene source, and air was used as an oxygen source (nitrogen in air served as a carrier gas). Prior to the catalytic reaction, the catalyst was pretreated with air at 470 °C for 1 h. The catalytic reaction was carried out at 420 °C. GHSV was fixed at 300 h<sup>-1</sup> on the basis of *n*-butene. Reaction products were periodically sampled and analyzed with a gas chromatography. Conversion of *n*-butene and selectivity for 1,3-butadiene were calculated on the basis of carbon balance as followings. Yield for 1,3-butadiene was calculated by multiplying conversion and selectivity.

$$\text{Conversion of } n\text{-butene} = \frac{\text{moles of } n\text{-butene reacted}}{\text{moles of } n\text{-butene supplied}}$$

$$\text{Selectivity for 1,3-butadiene} = \frac{\text{moles of 1,3-butadiene formed}}{\text{moles of } n\text{-butene reacted}}$$

## 3. Results and discussion

### 3.1. Characteristics of prepared catalysts

Formation of  $\alpha$ -Bi<sub>2</sub>Mo<sub>3</sub>O<sub>12</sub>,  $\beta$ -Bi<sub>2</sub>Mo<sub>2</sub>O<sub>9</sub>, and  $\gamma$ -Bi<sub>2</sub>MoO<sub>6</sub> catalysts was well confirmed by XRD, Raman spectroscopy, and ICP-AES measurements. Fig. 1 shows the XRD patterns and Raman spectra of prepared bismuth molybdate catalysts. These XRD patterns and Raman spectra were well consistent with those reported in previous works [7,14,20–22], indicating

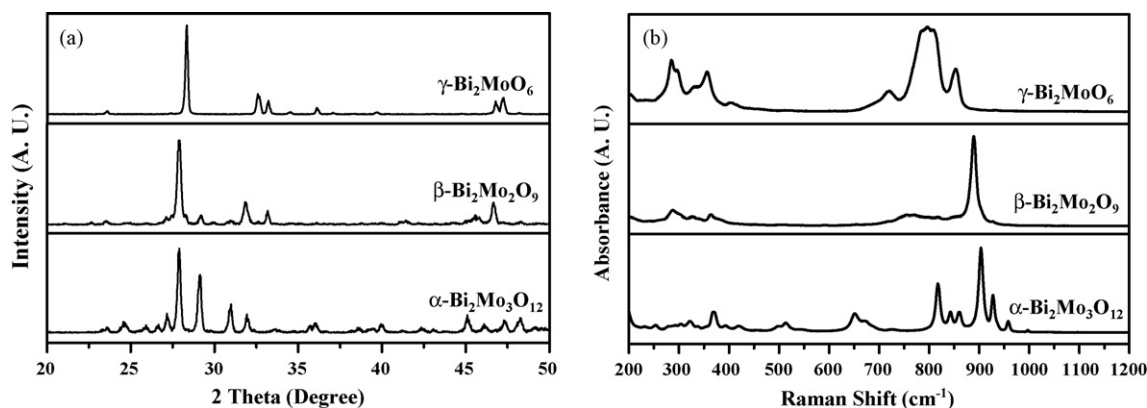


Fig. 1. (a) XRD patterns and (b) Raman spectra of prepared bismuth molybdate catalysts.

Table 1  
Bi/Mo atomic ratios and surface areas of prepared catalysts

Catalyst	Bi/Mo atomic ratio	BET surface area (m <sup>2</sup> /g)
$\alpha$ -Bi <sub>2</sub> Mo <sub>3</sub> O <sub>12</sub>	0.6	1.9
$\beta$ -Bi <sub>2</sub> Mo <sub>2</sub> O <sub>9</sub>	0.98	2.9
$\gamma$ -Bi <sub>2</sub> MoO <sub>6</sub>	1.96	3.5

successful formation of  $\alpha$ -Bi<sub>2</sub>Mo<sub>3</sub>O<sub>12</sub>,  $\beta$ -Bi<sub>2</sub>Mo<sub>2</sub>O<sub>9</sub>, and  $\gamma$ -Bi<sub>2</sub>MoO<sub>6</sub> catalysts. Bi/Mo atomic ratios and BET surface areas of prepared catalysts are summarized in Table 1. Bi/Mo atomic ratios of  $\alpha$ -Bi<sub>2</sub>Mo<sub>3</sub>O<sub>12</sub>,  $\beta$ -Bi<sub>2</sub>Mo<sub>2</sub>O<sub>9</sub>, and  $\gamma$ -Bi<sub>2</sub>MoO<sub>6</sub> were measured to be 0.6, 0.98, and 1.96, respectively. These values are in good agreement with the theoretical values (Bi/Mo = 2/3 for  $\alpha$ -Bi<sub>2</sub>Mo<sub>3</sub>O<sub>12</sub>, Bi/Mo = 1 for  $\beta$ -Bi<sub>2</sub>Mo<sub>2</sub>O<sub>9</sub>, and Bi/Mo = 2 for  $\gamma$ -Bi<sub>2</sub>MoO<sub>6</sub>). This result also supports that bismuth molybdate catalysts were successfully prepared in this work. BET surface areas of bismuth molybdate catalysts were found to be very low (ca. 2.0–4.0 m<sup>2</sup>/g), as reported in literatures [6,14,23].

### 3.2. Thermal stability of catalysts

Thermal stability of  $\alpha$ -Bi<sub>2</sub>Mo<sub>3</sub>O<sub>12</sub>,  $\beta$ -Bi<sub>2</sub>Mo<sub>2</sub>O<sub>9</sub>, and  $\gamma$ -Bi<sub>2</sub>MoO<sub>6</sub> catalysts was examined by XRD measurements. For this purpose, all the catalysts were thermally treated at 420 °C for 48 h in an air stream. Fig. 2 shows the XRD patterns of  $\alpha$ -Bi<sub>2</sub>Mo<sub>3</sub>O<sub>12</sub>,  $\beta$ -Bi<sub>2</sub>Mo<sub>2</sub>O<sub>9</sub>, and  $\gamma$ -Bi<sub>2</sub>MoO<sub>6</sub> catalysts obtained before and after the thermal treatment. It was observed that  $\alpha$ -Bi<sub>2</sub>Mo<sub>3</sub>O<sub>12</sub> and  $\gamma$ -Bi<sub>2</sub>MoO<sub>6</sub> catalysts showed no difference in XRD patterns before and after the thermal treatment, indicating

that  $\alpha$ -Bi<sub>2</sub>Mo<sub>3</sub>O<sub>12</sub> and  $\gamma$ -Bi<sub>2</sub>MoO<sub>6</sub> catalysts are thermally stable during the catalytic reaction performed at 420 °C. However,  $\beta$ -Bi<sub>2</sub>Mo<sub>2</sub>O<sub>9</sub> catalyst exhibited different XRD patterns before and after the thermal treatment. This means that  $\beta$ -Bi<sub>2</sub>Mo<sub>2</sub>O<sub>9</sub> catalyst is thermally unstable at the reaction temperature of 420 °C [7,13].

In order to ensure the thermal decomposition behavior of  $\beta$ -Bi<sub>2</sub>Mo<sub>2</sub>O<sub>9</sub>,  $\beta$ -Bi<sub>2</sub>Mo<sub>2</sub>O<sub>9</sub> catalyst was treated at 420 °C in an air stream with the variation of thermal treatment time. Fig. 3 shows the XRD patterns and Raman spectra of  $\beta$ -Bi<sub>2</sub>Mo<sub>2</sub>O<sub>9</sub> obtained with the variation of thermal treatment time at 420 °C. What is noticeable is that  $\alpha$ -Bi<sub>2</sub>Mo<sub>3</sub>O<sub>12</sub> and  $\gamma$ -Bi<sub>2</sub>MoO<sub>6</sub> phases appeared with increasing thermal treatment time. A close looking at the Raman spectra in Fig. 3 revealed that  $\beta$ -Bi<sub>2</sub>Mo<sub>2</sub>O<sub>9</sub> started to decompose after a certain period of thermal treatment (after 12 h). In order to quantify the degree of decomposition of  $\beta$ -Bi<sub>2</sub>Mo<sub>2</sub>O<sub>9</sub>, the strongest XRD and Raman peaks of  $\alpha$ -Bi<sub>2</sub>Mo<sub>3</sub>O<sub>12</sub>,  $\beta$ -Bi<sub>2</sub>Mo<sub>2</sub>O<sub>9</sub>, and  $\gamma$ -Bi<sub>2</sub>MoO<sub>6</sub> phases in the thermally decomposed  $\beta$ -Bi<sub>2</sub>Mo<sub>2</sub>O<sub>9</sub> were identified, and then their intensity ratios were calculated for the precise quantification according to the method in literature [24]. In the calculations, it was assumed that 2 mol of  $\beta$ -Bi<sub>2</sub>Mo<sub>2</sub>O<sub>9</sub> were decomposed into 1 mol of  $\alpha$ -Bi<sub>2</sub>Mo<sub>3</sub>O<sub>12</sub> and 1 mol of  $\gamma$ -Bi<sub>2</sub>MoO<sub>6</sub> [24]. Table 2 summarizes the degree of decomposition of  $\beta$ -Bi<sub>2</sub>Mo<sub>2</sub>O<sub>9</sub> with the variation of thermal treatment time at 420 °C. Quantification for the degree of decomposition of  $\beta$ -Bi<sub>2</sub>Mo<sub>2</sub>O<sub>9</sub> after 12 and 18 h was not a simple task due to the weak peak intensities. Table 2 shows that ca. 55 and 70% of  $\beta$ -Bi<sub>2</sub>Mo<sub>2</sub>O<sub>9</sub> were decomposed into  $\alpha$ -Bi<sub>2</sub>Mo<sub>3</sub>O<sub>12</sub> and  $\gamma$ -Bi<sub>2</sub>MoO<sub>6</sub> after 24 and 48 h, respectively. This result implies that  $\beta$ -Bi<sub>2</sub>Mo<sub>2</sub>O<sub>9</sub> cannot

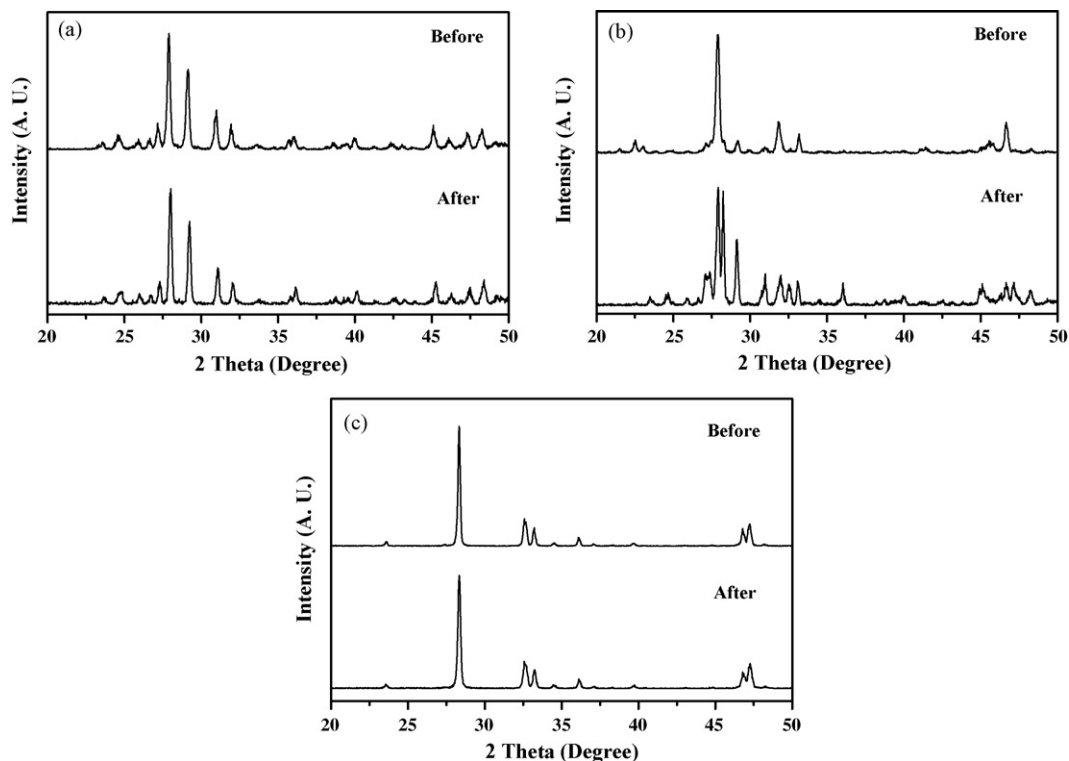


Fig. 2. XRD patterns of (a)  $\alpha$ -Bi<sub>2</sub>Mo<sub>3</sub>O<sub>12</sub>, (b)  $\beta$ -Bi<sub>2</sub>Mo<sub>2</sub>O<sub>9</sub>, and (c)  $\gamma$ -Bi<sub>2</sub>MoO<sub>6</sub> obtained before and after the thermal treatment at 420 °C for 48 h.

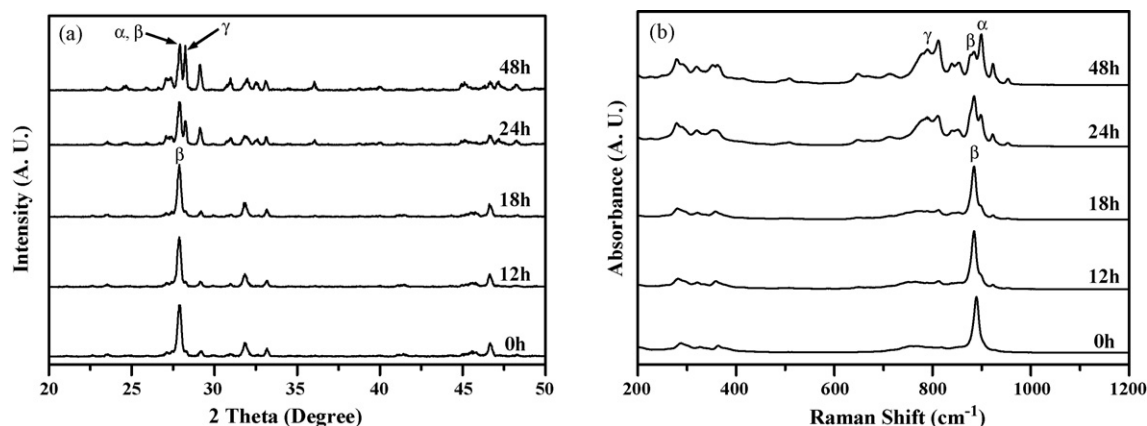


Fig. 3. (a) XRD patterns and (b) Raman spectra of  $\beta$ - $\text{Bi}_2\text{Mo}_2\text{O}_9$  obtained with the variation of thermal treatment time at  $420^\circ\text{C}$ .

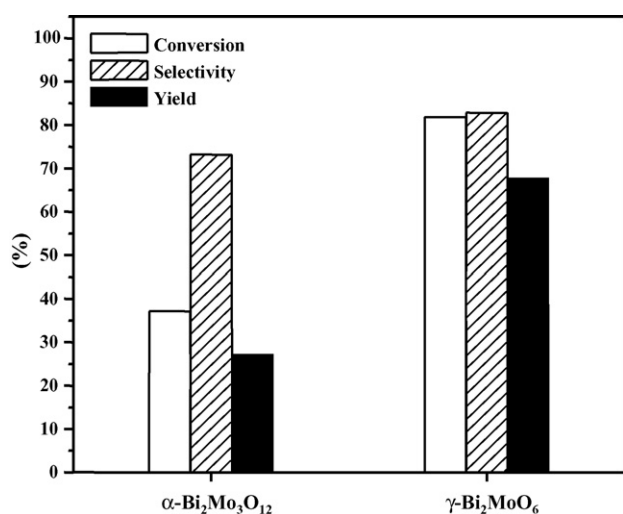


Fig. 4. Catalytic performance of  $\alpha$ - $\text{Bi}_2\text{Mo}_3\text{O}_{12}$  and  $\gamma$ - $\text{Bi}_2\text{MoO}_6$  in the oxidative dehydrogenation of *n*-butene at  $420^\circ\text{C}$  after 48 h.

serve as an efficient catalyst in the oxidative dehydrogenation of *n*-butene performed at  $420^\circ\text{C}$ . In this work, therefore,  $\beta$ - $\text{Bi}_2\text{Mo}_2\text{O}_9$  was excluded in the catalytic performance tests.

### 3.3. Catalytic performance in the oxidative dehydrogenation of *n*-butene

Fig. 4 shows the catalytic performance of  $\alpha$ - $\text{Bi}_2\text{Mo}_3\text{O}_{12}$  and  $\gamma$ - $\text{Bi}_2\text{MoO}_6$  in the oxidative dehydrogenation of *n*-butene at  $420^\circ\text{C}$  after 48 h. Conversion of *n*-butene and selectivity for

1,3-butadiene obtained with  $\gamma$ - $\text{Bi}_2\text{MoO}_6$  catalyst were much higher than those obtained with  $\alpha$ - $\text{Bi}_2\text{Mo}_3\text{O}_{12}$  catalyst. As a consequence,  $\gamma$ - $\text{Bi}_2\text{MoO}_6$  catalyst exhibited a higher yield for 1,3-butadiene than  $\alpha$ - $\text{Bi}_2\text{Mo}_3\text{O}_{12}$  catalyst. In order to verify the different catalytic performance between  $\alpha$ - $\text{Bi}_2\text{Mo}_3\text{O}_{12}$  and  $\gamma$ - $\text{Bi}_2\text{MoO}_6$  catalysts, TPRO experiments were carried out with an aim of measuring the oxygen mobility in both catalysts.

At first, oxidative dehydrogenation of *n*-butene was carried out in the absence of oxygen feed at  $420^\circ\text{C}$  for 3 h in order for the catalyst to consume lattice oxygens for the reaction. Table 3 summarizes the catalytic performance of  $\alpha$ - $\text{Bi}_2\text{Mo}_3\text{O}_{12}$  and  $\gamma$ - $\text{Bi}_2\text{MoO}_6$  in the presence or absence of oxygen feed at  $420^\circ\text{C}$  after 3 h. As listed in Table 3, both  $\alpha$ - $\text{Bi}_2\text{Mo}_3\text{O}_{12}$  and  $\gamma$ - $\text{Bi}_2\text{MoO}_6$  catalysts in the absence of oxygen feed exhibited comparable catalytic activities to those in the presence of oxygen feed. This means that both catalysts consumed lattice oxygens for the reaction in the absence of oxygen feed [6,14–18]. TPRO experiments were conducted with partially reduced catalysts obtained in the absence of oxygen feed. Fig. 5 shows the TPRO profiles of partially reduced  $\alpha$ - $\text{Bi}_2\text{Mo}_3\text{O}_{12}$  and  $\gamma$ - $\text{Bi}_2\text{MoO}_6$  catalysts. The amount of oxygen consumption measured by TPRO experiment is equivalent to the amount of oxygen vacancy in the partially reduced catalyst. The peak representing make-up oxygen in the  $\gamma$ - $\text{Bi}_2\text{MoO}_6$  appeared at low temperature region ( $150$ – $300^\circ\text{C}$ ), while that in the  $\alpha$ - $\text{Bi}_2\text{Mo}_3\text{O}_{12}$  appeared at high temperature region ( $300$ – $450^\circ\text{C}$ ). Although, both  $\alpha$ - $\text{Bi}_2\text{Mo}_3\text{O}_{12}$  and  $\gamma$ - $\text{Bi}_2\text{MoO}_6$  catalysts showed the maximum TPRO peaks below the reaction temperature of  $420^\circ\text{C}$ , one should compare the oxygen mobility on the basis of relative TPRO peak position because the TPRO profiles vary depending on the experimental

Table 2

Degree of decomposition of  $\beta$ - $\text{Bi}_2\text{Mo}_2\text{O}_9$  with the variation of thermal treatment time at  $420^\circ\text{C}$

Thermal treatment time (h)	Composition distribution calculated from XRD data			Composition distribution calculated from Raman data		
	$\alpha$ (%)	$\beta$ (%)	$\gamma$ (%)	$\alpha$ (%)	$\beta$ (%)	$\gamma$ (%)
0	0	100	0	0	100	0
12	–	100	–	–	100	–
18	–	100	–	–	100	–
24	26.5	47	26.5	28	44	28
48	33	34	33	37.5	25	37.5

Table 3  
Catalytic performance of  $\alpha$ - $\text{Bi}_2\text{Mo}_3\text{O}_{12}$  and  $\gamma$ - $\text{Bi}_2\text{MoO}_6$  in the presence or absence of oxygen feed at 420 °C after 3 h

Catalyst	With oxygen feed			Without oxygen feed		
	Conversion (%)	Selectivity (%)	Yield (%)	Conversion (%)	Selectivity (%)	Yield (%)
$\alpha$ - $\text{Bi}_2\text{Mo}_3\text{O}_{12}$	37.2	73.2	27.2	30.0	84.1	25.2
$\gamma$ - $\text{Bi}_2\text{MoO}_6$	81.8	82.8	67.7	77.0	87.8	67.6

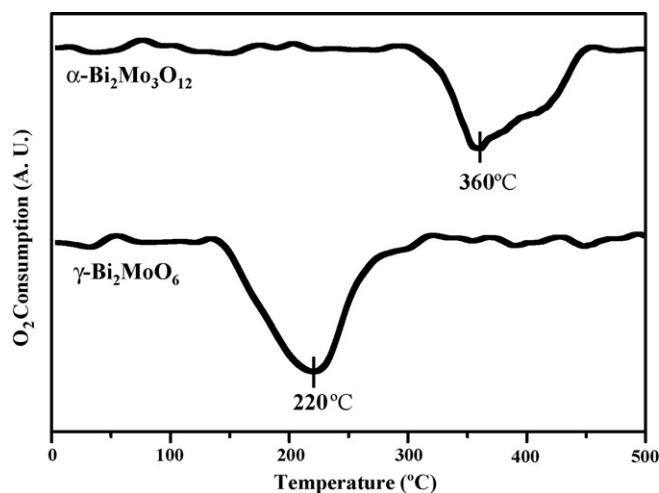


Fig. 5. TPRO profiles of partially reduced  $\alpha$ - $\text{Bi}_2\text{Mo}_3\text{O}_{12}$  and  $\gamma$ - $\text{Bi}_2\text{MoO}_6$  catalysts.

conditions such as heating rate and feed flow rate. In the TPRO measurements, the lower TPRO peak temperature corresponds to the higher oxygen mobility. The above result strongly supports that  $\gamma$ - $\text{Bi}_2\text{MoO}_6$  catalyst retains higher oxygen mobility than  $\alpha$ - $\text{Bi}_2\text{Mo}_3\text{O}_{12}$  catalyst. Therefore, it is concluded that the enhanced catalytic performance of  $\gamma$ - $\text{Bi}_2\text{MoO}_6$  was attributed to the facile oxygen mobility of  $\gamma$ - $\text{Bi}_2\text{MoO}_6$ .

#### 4. Conclusions

$\alpha$ - $\text{Bi}_2\text{Mo}_3\text{O}_{12}$ ,  $\beta$ - $\text{Bi}_2\text{Mo}_2\text{O}_9$ , and  $\gamma$ - $\text{Bi}_2\text{MoO}_6$  catalysts were prepared by a co-precipitation method for use in the oxidative dehydrogenation of *n*-butene. Formation of  $\alpha$ - $\text{Bi}_2\text{Mo}_3\text{O}_{12}$ ,  $\beta$ - $\text{Bi}_2\text{Mo}_2\text{O}_9$ , and  $\gamma$ - $\text{Bi}_2\text{MoO}_6$  catalysts was well confirmed by XRD, Raman spectroscopy, and ICP-AES analyses. It was found that  $\beta$ - $\text{Bi}_2\text{Mo}_2\text{O}_9$  was thermally unstable and decomposed into  $\alpha$ - $\text{Bi}_2\text{Mo}_3\text{O}_{12}$  and  $\gamma$ - $\text{Bi}_2\text{MoO}_6$  at the reaction temperature of 420 °C, and therefore,  $\beta$ - $\text{Bi}_2\text{Mo}_2\text{O}_9$  could not serve as an effi-

cient catalyst in the reaction. In the oxidative dehydrogenation of *n*-butene, it was revealed that  $\gamma$ - $\text{Bi}_2\text{MoO}_6$  showed a better catalytic performance than  $\alpha$ - $\text{Bi}_2\text{Mo}_3\text{O}_{12}$  due to the facile oxygen mobility of  $\gamma$ - $\text{Bi}_2\text{MoO}_6$ .

#### Acknowledgement

The authors acknowledge the support from Korea Energy Management Corporation (2005-01-0090-3-010).

#### References

- [1] S.C. Oh, H.P. Lee, H.T. Kim, K.O. Yoo, Korean J. Chem. Eng. 16 (1999) 543.
- [2] L.M. Madeira, M.F. Portela, Catal. Rev. 44 (2002) 247.
- [3] H.H. Kung, Adv. Catal. 40 (1994) 1.
- [4] M.A. Chaar, K. Patel, H.H. Kung, J. Catal. 109 (1988) 463.
- [5] E.A. Mamedov, V.C. Corberán, Appl. Catal. A 127 (1995) 1.
- [6] A.P.V. Soares, L.D. Dimitrov, M.C.A. Oliveira, L. Hilaire, M.F. Portela, R.K. Grasselli, Appl. Catal. A 253 (2003) 191.
- [7] Ph.A. Batist, J.F.H. Bouwens, G.C.A. Schuit, J. Catal. 25 (1972) 1.
- [8] R.K. Grasselli, Topics Catal. 21 (2002) 79.
- [9] W.J. Linn, A.W. Sleight, J. Catal. 41 (1976) 134.
- [10] Ph.A. Batist, B.C. Lippens, G.C.A. Schuit, J. Catal. 5 (1966) 55.
- [11] A.C.A.M. Bleijenberg, B.C. Lippens, G.C.A. Schuit, J. Catal. 4 (1965) 581.
- [12] M. Egashira, K. Matsuo, S. Kagawa, T. Seiyama, J. Catal. 58 (1979) 409.
- [13] B. Grzybowska, J. Haber, J. Komorek, J. Catal. 25 (1972) 25.
- [14] Ph.A. Batist, A.H.W.M. Der Kinderen, Y. Leeuwenburgh, F.A.M.G. Metz, G.C.A. Schuit, J. Catal. 12 (1968) 45.
- [15] E. Ruckenstein, R. Krishnan, K.N. Rai, J. Catal. 45 (1976) 270.
- [16] M.F. Portela, Topics Catal. 15 (2001) 241.
- [17] Y.M. Oka, W. Ueda, Adv. Catal. 40 (1994) 233.
- [18] R.K. Grasselli, Handbook of Heterogeneous Catalysis, Wiley Publishing, New York, 1997.
- [19] G.W. Keulks, J.L. Hall, C. Daniel, K. Suzuki, J. Catal. 34 (1974) 79.
- [20] E.V. Hoefs, J.R. Monnier, G.W. Keulks, J. Catal. 57 (1979) 331.
- [21] B. Grzybowska, J. Haber, W. Marczewski, L. Ungier, J. Catal. 42 (1976) 327.
- [22] P. Boutry, R. Montarnal, J. Wrzyszczyk, J. Catal. 13 (1969) 75.
- [23] L.D. Krenzke, G.W. Keulks, J. Catal. 64 (1980) 295.
- [24] M.T. Le, W.J.M. Van Well, P. Stoltze, I. Van Driessche, S. Hoste, Appl. Catal. A 282 (2005) 189.